Fluid Dynamics, Vol 34, No. 1, 1999

NONLOCAL TURBULENT TRANSPORT IN A BUOYANT VORTEX RING DURING THE ASCENT OF A THERMAL IN A STRATIFIED ATMOSPHERE

A. V. Konyukhov, M. V. Meshcheryakov, S. V. Utyuzhnikov, and L. A. Chudov

UDC 532 517.4:536.24

The flow initiated by a hot gas cloud (thermal) in a stratified atmosphere is calculated on the basis of the k–ε turbulence model and the transport model for the Reynolds stresses and turbulent fluxes and the results obtained are compared The nonlocal nature of the turbulent transport in a vortex ring and its effect on certain flow characteristics are explained In particular, the calculations carried out using the Reynolds stress model show much slower cooling of the temperature-vortex torus than those based calculated on the k–ε-model Modification of the k–ε-model to take the effect of curvature of the streamlines approximately into account makes it only partially possible to reproduce the results obtained on the basis of the Reynolds stress model

The ascent of an atmospheric thermal is accompanied by the rolling up of the gas into a vortex ring. It is difficult to calculate the turbulent transport in the vortex ring and its effect on the average flow characteristics, in particular, on the temperature-vortex torus cooling rate. On the one hand, the flow is turbulent. This is observable from the presence of large-scale vortex structures and the developed turbulent spectrum in laboratory and full-scale experiments. On the other hand, the stabilizing action of rotation on the turbulence in the core of the vortex ring and the suppression of radial turbulent heat transport has been established experimentally and theoretically [1–3].

Local turbulence models using the Boussinesq hypothesis on the coincidence of the principal axes of the Reynolds stress tensor (fluxes) and the average strain-rate tensor (gradient of average quantities) were applied to the problem of the ascent of a turbulent thermal transformed during its motion into a buoyant vortex ring in, for example, [4, 5], where the k–ε turbulence model was used for calculating the ascending thermal. As compared with algebraic models, the differential models make it possible more fully to simulate the turbulence scale and the unsteadiness of the flow since the turbulent time scale is of the same order as the characteristic time of variation of the average flow characteristics. In [4] a combined model which proposed different turbulent transport coefficients along the radius of the vortex and in the perpendicular direction was used to calculate the turbulent transport in a buoyant vortex ring initiated by a thermal. In [6], where the k–ε-model was also used, strong cooling of the turbulent thermal was obtained as compared with the inviscid model calculations.

Below, this characteristic is used to compare the calculation results obtained on the basis of the k–ε-model and the differential model for the Reynolds stresses in which the Boussinesq hypothesis is rejected. In [1] the Reynolds stress model was used to calculate the damping of a plane atmospheric vortex. In the present paper, this model makes it possible to assess the applicability of the physical hypotheses of turbulent transport in the complex flow in question from the standpoint of a more general theory. For the purpose of determining the effect of the vorticity of the flow on the turbulent stresses and fluxes, the stress model is realized in the form proposed in [7]. In the model equations the deformation components of the generation and redistribution of stresses and fluxes are taken into account and the components taking the buoyancy forces into account are omitted. The contribution of the buoyancy forces in the thermal to the turbulent transport is comparable with that of the rotation forces. Nevertheless, the effect of the former on the turbulent transport was not taken into account. This made it possible separately to investigate the effect of the anisotropy due to the influence of the centrifugal forces in the vortex ring. The experimental results and the numerical simulation of the contragradient transport phenomena were described in detail in [8].

1. We will consider the model problem of the ascent of an individual large-scale hot gas cloud (thermal) in an inhomogeneous atmosphere [4–6, 9]. At the initial instant the static pressure throughout the entire computational domain is assumed to be equal to the atmospheric pressure at a height z above sea level. Outside a spherical volume of radius $R_0=1$ km the temperature (density) distribution corresponds to atmospheric, and inside the thermal the gas temperature is $T_0=900$ K. Initially, the centre of the spherical volume is located above the ground surface at a height $H_0=3$ km. In this formulation we can say that the underlying surface does not affect the resulting flow. The dimensions of the computational domain (in which the left boundary corresponds to the axis of symmetry) are 6 km in the radial

Moscow. Translated from Izvestiya Rossiiskoi Akademii Nauk, Mekhanika Zhidkosti i Gaza, No. 1, pp. 12–20, January–February, 1999. Original article submitted May 13, 1997.

0015-4628/99/3401-0009$22.00

direction and 15 km in height. The initial gas velocity is assumed to be equal to zero throughout the entire domain. The standard atmosphere model [5] was used in the calculations.

2. In orthogonal coordinates the system of equations of motion of the gas can be written in the form:

$$\frac{\partial \rho}{\partial t} + \nabla\cdot(\rho \mathbf{V}) = 0$$

$$\frac{\partial \rho \mathbf{V}}{\partial t} + \nabla\cdot(\rho \mathbf{V}\mathbf{V} + p\mathbf{I} - \mathbf{R}) = \rho \mathbf{g}$$

$$\frac{\partial \rho E}{\partial t} + \nabla\cdot\left(\rho \mathbf{V}\left(E + \frac{p}{\rho}\right) - \mathbf{R}\cdot\mathbf{V} + \mathbf{q}\right) = \rho \mathbf{g}\mathbf{V}$$

$$E = e + \frac{\mathbf{V}\cdot\mathbf{V}}{2}, \quad k = \frac{1}{2}\langle u_l u_l\rangle, \quad R_{ij} = -\rho\langle u_i u_j\rangle, \quad q_i = -\rho\langle u_i h\rangle \tag{2.1}$$

$$\mathbf{q} = -\gamma \mu_t \nabla e$$

$$\mathbf{R} = -\frac{2}{3}(\rho k + \mu_t \nabla\mathbf{V})\mathbf{I} + 2\mu_t \mathbf{S}$$

$$S_{ij} = \frac{1}{2}(\nabla_i v_j + \nabla_j v_i)$$

Here, e is the intrinsic energy of the gas, $\mathbf{q}$ is the turbulent heat flux, h is the enthalpy fluctuation, $\mathbf{g}$ is the gravity field vector, and $\mathbf{S}$ is the strain-rate tensor.

The system (2.1) is closed using the Boussinesq hypothesis on the basis of the k–ε turbulence model for a perfect gas and with allowance for the Kolmogorov-Prandtl formula

$$\frac{\partial \rho k}{\partial t} + \nabla\cdot(\rho \mathbf{V} k - D_k \nabla k) = P - \rho\varepsilon$$

$$\frac{\partial \rho \varepsilon}{\partial t} + \nabla\cdot(\rho \mathbf{V}\varepsilon - D_\varepsilon \nabla\varepsilon) = (c_{1\varepsilon} P - c_{2\varepsilon} f_2 \rho\varepsilon)\frac{\varepsilon}{k} \tag{2.2}$$

$$D_k = \frac{\mu_t}{\sigma_k}, \quad D_\varepsilon = \frac{\mu_t}{\sigma_\varepsilon}, \quad P = R_{kl} V_{k,l} = -\rho\langle u_k u_l\rangle V_{k,l}$$

$$\mu_t = c_\mu f_\mu \rho \frac{k^2}{\varepsilon}$$

In (2.2) the values of the constants are

$$c_\mu = 0.09, \quad c_{1\varepsilon} = 1.45, \quad c_{2\varepsilon} = 1.90, \quad \sigma_k = 1.0, \quad \sigma_\varepsilon = 1.3$$

In the absence of corrections for rotation the values of the constants f_2 and f_μ were equal to unity. Within the framework of the k–ε model the flow anisotropy in the thermal due to the action of the centrifugal forces in the vortex ring was taken into account by introducing the coefficients f_2 and f_μ. This modification of the model was called the nonlinear k–ε model (see, for example, [10]). The following expressions were used for the correction coefficients [11]:

$$f_2 = (1 - 0.2\,\mathrm{Ri}_c), \quad \mathrm{Ri}_c = \frac{k^2}{\varepsilon^2}\frac{V_s}{R_c^2}\frac{\partial(V_s R_c)}{\partial R_c}$$

$$f_\mu = \left[1 + 8k_1^2\frac{k^2}{\varepsilon^2}\left(\frac{\partial V_s}{\partial n} + \frac{V_s}{R_c}\right)\frac{V_s}{R_c}\right]^{-1}, \quad k_1 = 0.27$$

Here, Ri_c is the Richardson number, V_s is the instantaneous velocity component, R_c is the radius of curvature of the streamlines, and $\mathbf{n}$ is the streamline normal.

The system of equations of the Reynolds stress transport model can be written in the form:

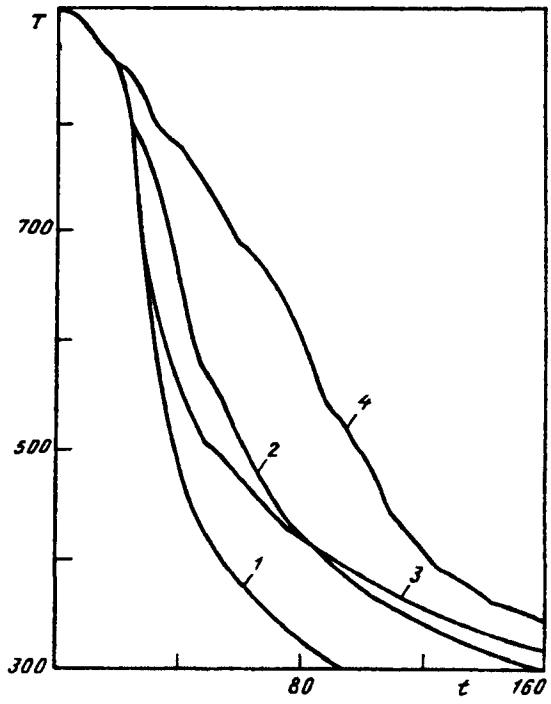

Fig. 1. Time (in s) dependence of the maximum temperature (in K) in the thermal; curves *1–4* correspond to the k–ε, nonlinear k–ε, Reynolds-stress, and inviscid models, respectively.

$$\frac{\partial \rho \langle u_i u_j \rangle}{\partial t} + \nabla \cdot (\rho \langle u_i u_j \rangle \mathbf{V}) - \mathrm{diff}(\langle u_i u_j \rangle) = P_{ij} + \Phi_{ij}^1 + \Phi_{ij}^2 - \rho \varepsilon_{ij}$$

$$\frac{\partial \rho \langle u_i e \rangle}{\partial t} + \nabla \cdot (\rho \langle u_i e \rangle \mathbf{V}) - \mathrm{diff}(\langle u_i e \rangle) = P_{ie} + \Phi_{ie}$$

$$\frac{\partial \rho \varepsilon}{\partial t} + \nabla \cdot (\rho \mathbf{V} \varepsilon) - \mathrm{diff}(\varepsilon) = (c_{1\varepsilon} P - c_{2\varepsilon} \rho \varepsilon) \frac{\varepsilon}{k}$$

$$P_{ij} = -\rho \langle u_i u_k \rangle V_{j,k} - \rho \langle u_j u_k \rangle V_{i,k}$$

$$\Phi_{ij}^1 = -\rho c_1 \frac{\varepsilon}{k} \left(\langle u_i u_j \rangle - \frac{2}{3} k \delta_{ij} \right)$$

$$\Phi_{ij}^2 = -\alpha \left(P_{ij} - \frac{2}{3} P \delta_{ij} \right) - \beta \rho k (V_{i,j} + V_{j,i}) - \gamma \left(D_{ij} - \frac{2}{3} P \delta_{ij} \right)$$

$$P_{ie} = -\rho \langle u_{ie} e \rangle V_{ie} - \rho \langle u_m e \rangle V_{mi}, \qquad \Phi_{ie} = -c_{1e} \rho \frac{\varepsilon}{k} \langle u_i e \rangle + c_{2e} \rho \langle u_l e \rangle V_{i,l}$$

$$D_{ij} = -\rho \langle u_i u_k \rangle V_{kj} - \rho \langle u_j u_k \rangle V_{k,i}, \qquad \varepsilon_{ij} = 2/3\, \varepsilon\, \delta_{ij}$$

$$\mathrm{diff}(\langle u_i u_j \rangle) = -c_s (\rho \langle u_l u_k \rangle \langle u_i u_j \rangle)_{,k})_{,l}, \qquad \mathrm{diff}(\varepsilon) = -c_s (\rho \langle u_l u_k \rangle \varepsilon_{,k})_{,l}$$

The constants have the values

$$c_1 = 1.8, \quad \alpha = 0.764, \quad \beta = 0.182, \quad \gamma = 0.109, \quad c_s = 0.11, \quad c_\varepsilon = 0.15,$$

$$c_{1\varepsilon} = 1.44, \quad c_{2\varepsilon} = 1.92, \quad c_{1e} = 3.0, \quad c_{2e} = 0.33$$

The initial data for the variables k and ε (here, k is the kinetic energy of the turbulent fluctuations and ε is its dissipation rate) were determined using the methods described in [5, 12]. The time of transition from the inviscid model to the k–ε model was taken equal to the time required for the thermal to be rolled up into a vortex ring (t_0=4.5 s). The values of k and ε corresponding to the approximation of balanced generation, dissipation and diffusion processes were taken as the initial data. At the initial instant the integral turbulent lengthscale was set equal to $0.1R_0$ [5, 10]. When the Reynolds stress model was used, the initial date for k and ε were similarly specified. The initial Reynolds stress tensor was assumed to be spherical, so that $\langle u_1u_1\rangle=\langle u_2u_2\rangle=\langle u_3u_3\rangle=\frac{1}{3}k$.

At the initial instant a "passive" admixture consisting of a fixed number of marker-particles was distributed over the thermal. This admixture was used for determining certain geometric characteristics of the flow. In addition, trajectories of four individual particles were specially traced.

The finite-difference grid contained 101×201 node points and was spatially uniform. The numerical solution was found using a TVD scheme [13] modified to ensure second-order time approximation. The parameters of the inviscid thermal were in good agreement with the calculation results obtained by means of the "leap-frog" scheme [14]. The corresponding computational program was tested in some detail by checking the dependence on the grid step and the fulfilment of the integral conservation laws [5, 6]. In the calculations the Courant number was set equal to 0.5 (with a gradual increase to 1.5 in the course of the calculations).

4. We considered four model variants: (1) Euler equations; (2) standard k–ε-model; (3) nonlinear k–ε-model (in what follows denoted model 3); Reynolds stress model (model 4).

The basic laws of the developing flow are well known; nevertheless, the question of the mechanism of realization of the turbulence effects and the determination of their spatial and time zones of maximum manifestation remains open [6].

For the given parameters of the thermal the vortex ring is formed by the instant t=5 s, which determined the cut-in time for the turbulent models.

In Fig. 1 we have plotted graphs of the time dependence of the maximum temperature which illustrate the effect of turbulent transport on the thermal cooling rate. The calculations based on model 4 indicate much slower cooling of the temperature-vortex torus than those based on the k–ε-model. In this case, up to 45 s the k–ε-model gives results closer to those of model 4 than the results obtained on the basis of model 3. According to [10, 15], the terms in the equations for the turbulent heat flux (omitted in our analysis), which express the work done by the turbulent fluctuations of the inertia force field, tend to weaken the turbulent heat transfer in the radial direction in the vortex ring, i.e., add to the difference between the results of the k–ε-model and model 4.

We note that up to the instant t=25 s the time dependences of the maximum temperature almost coincide for all the variants, after which the curves obtained on the basis of the k–ε-model and model 4 drop sharply with respect to those obtained in the inviscid calculation. This time interval from 25 s to 40 s is characterized by the transformation of the thermal into a torus. By the instant t=40 s this process can be considered to be already complete. From the instant t=60 s curve 3 corresponding to model 4 lies above curve 2 (model 3).

Despite significant differences between the time dependences of the maximum temperature for the different models, the coordinates of the point of maximum temperature almost coincide for all the variants.

A characteristic of the graphs of the time dependence of the maximum vorticity is the presence of a local maximum at t~15–20 s corresponding to transformation of the thermal into a torus and the principal maximum at t~40–50 s. The values of the principal and local maxima are equal to 0.97, 0.56, 0.76, and 0.62 and 0.37, 0.52, 0.6, and 0.52 for models 1–4, respectively. Hence it is clear that model 3 gives overestimated values of the vorticity.

The time dependences of the height of the vorticity maximum coincide for all the variants. Starting from t=180 s the curves of the radius of maximum vorticity as functions of time begin to diverge, the radius of the vortex ring increasing more strongly for models 1 and 4 and more slowly for the k–ε-model. For example, by the time t=300 s the radius of the vortex ring is 4.85, 3.96, 4.4, and 5.16 km for variants 1–4, respectively. As a result, the trajectory of the maximum vorticity is steepest for the k–ε-model and flattest for model 4.

The time dependences of the height of the upper edge coincide for all the variants up to t=150 s (this corresponds to the so-called self-similar interval of ascent of the thermal). Then the curves for variants 2 and 1 lie, respectively, above and below all the other curves, but starting from t=236 s all three variants of the turbulent calculations result in the thermal hovering at the height H^*=13.6 km. At the same time, in the inviscid calculation the thermal continues to ascend, hovering at the height H^*=14.2 km at t=300 s.

The radius of the thermal front is characterized by the same relations between the variants as the radius of the center of the vortex ring. For example, at t=300 s the radii of the front are equal to 5.4, 4.3, 4.8, and 5.6 km for models 1–4, respectively.

We can also distinguish the maximum vertical and horizontal velocity components as quantities characterizing the dynamics of ascent of the thermal. In all the calculations the maximum vertical velocity is achieved at t=20 s and its

value lies on the interval from 200 m/s (for variant 1) to 182 m/s (for variant 4). The dependences of the maximum vertical velocity component as functions of t almost coincide up to $t=120$ s. After that they begin to deviate. For example, at time $t=300$ s they are equal to 96, 24, 60, and 76 m/s for variants 1–4, respectively.

The heights of the point with the maximum velocity almost coincide for all the calculations, but their radii differ as do the radii of the centers of the vortex ring. At $t=300$ s the radii of the points of maximum velocity are equal to 4.2, 2.6, 3.6, and 4.4 km for variants 1–4, respectively.

The horizontal velocity component has a maximum at $t=120$ s, the time dependences of the horizontal velocity coinciding for all the variants up to $t=70$ s and after that beginning to differ. At $t=200$ s the maxima of the positive values of the horizontal velocity component are equal to 92, 56, 68, and 80 m/s for variants 1–4, respectively. In this case the trajectories of the maximum points of the vertical and horizontal velocity components are steepest for the k–ε-model and flattest for the inviscid model and model 4. The corresponding graphs for model 4 and the inviscid model almost coincide. The curves of the maximum horizontal velocity component draw closer together at times $t > 300$ s. As distinct from the horizontal (radial) velocity component, the maximum absolute value of the negative vertical velocity component is less than the maximum positive component by approximately a factor of 3. On several time intervals the negative horizontal velocity component is 20–30% greater (in absolute value) than the positive component. This relates to times $t \sim 20$–100 s when the surrounding air flows into the thermal.

In our calculations we traced the time dependences of both the height and the radial coordinate of four particles in the thermal (located initially in the center, and at the lower, upper and right edges) and the trajectories of these particles. This made it possible to establish the basic laws of motion of admixture particles inside the ascending thermal. Moreover, the period of rotation of the vortex ring, equal to 70 s, was determined for variants 1, 3, and 4. This period was conserved throughout the motion of the thermal. For the k–ε-model the period was equal to 90 s and increased gradually, in particular, at $t > 220$ s. Thus, for the k–ε-model the rotation velocity of the vortex ring decreased most strongly on the hovering intervals. For variants 1 and 4 the period of revolution was almost constant and equal to $5.5(R_0/g)^{1/2}$, while for variant 2 the period continuously increased and exceeded the value $T=6(R_0/g)^{1/2}$. In Fig. 2 we have plotted graphs of the time dependence of the radial coordinate of a particle initially located at the upper edge of the thermal. One can clearly see the increase in the period of revolution of the vortex ring for the k–ε-model.

An analysis of the distributions of the quantities $\langle u^2\rangle$, $\langle v^2\rangle$, and $\langle w^2\rangle$ in the r-z plane at various instants of time shows that the turbulence strongly deviates from the isotropic state ($\langle u^2\rangle=\langle v^2\rangle=\langle w^2\rangle$). Here, u, v, and w are the turbulent fluctuation components in the cylindrical coordinates (r, z, φ). In order to estimate the applicability of the Boussinesq hypothesis for determining the turbulent friction stress $-\langle uv\rangle$ we will consider the solution obtained on the basis of model 4 at a time when the temperature-vortex torus is completely formed and the flow structure typical for the entire ascent stage.

In Fig. 3*a* we have reproduced the corresponding component of the strain-rate tensor $0.5(V_r + V_z)$ (here, U and V are the components of the average velocity along the r and z axes) at a point 80 s from the beginning of the motion, and in the Fig. 3*b* we have reproduced the distribution of the turbulent friction $-\langle uv\rangle$. In the local turbulent transport approximation the quantities considered coincide to within twice the turbulent viscosity coefficient. At the same time, in Fig. 3*b* there are regions 1 and 2 corresponding to a positive value of the quantity $\langle uv\rangle(v_r + u_z)$, i.e., a region of contragradient transport. It should be noted that in region 1 the value of the "antidiffuse" flux is fairly large, amounting to 30% (in absolute value) of the absolute maximum in the flow field. In regions 1 and 2 the term $-\langle uv\rangle(v_r + u_z)$ makes a negative contribution to the kinetic turbulence energy production. This should lead to a decrease in k as compared with the results for the k–ε-model. In fact, in Fig. 4 we have plotted graphs of the time dependence of the maximum kinetic turbulence energy, the lower curve corresponding to model 4. A comparison of the calculations based on model 4 and the k–ε-model shows that stratification of the $k(t)$ curves begins after the formation of the vortex ring at $t > 35$ s. This confirms the stabilizing effect of the rotation on the turbulence.

The nonlocal nature of the turbulent transport of scalar quantities can be seen from a comparison of the directions of the turbulent fluxes and the gradient of the corresponding quantity taken with the opposite sign at various points of the flow. In Fig. 5*a* we have reproduced the data for the temperature corresponding to $t=50$ s. The flow region enveloping the vortex ring is covered by a grid at the nodes of which we have reconstructed the turbulent heat flux vectors (with arrow heads) and the temperature gradient taken with the opposite sign (without arrow heads) divided by the maximum length in the flow field. The scalar product of these vectors is positive in the region of maximum shear stresses in the upper and outer parts of the vortex and negative inside (contragradient transport). Obviously, this is due to the rotation of the vortex ring, since at earlier instants of time ($t=30$ s, Fig. 5*b*, same notation), before the formation of the temperature-vortex torus, there is no contragradient transport region.

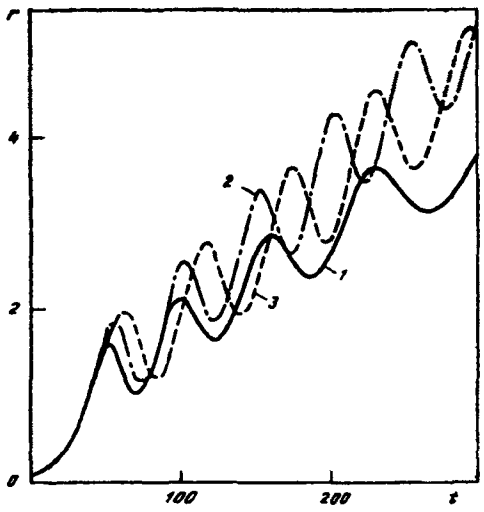

Fig. 2

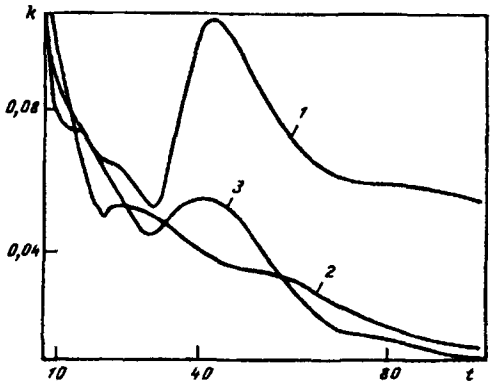

Fig. 4

Fig. 2. Time (in s) dependence of the radial coordinate (in km) of a marker particle; curves *1–3* correspond to the k–ε, nonlinear k–ε, and inviscid models, respectively.

Fig. 4. Time (in s) dependence of the maximum kinetic turbulence energy (in 10^6 m^2/s^2). The notation for curves *1–3* is the same as in Fig. 1.

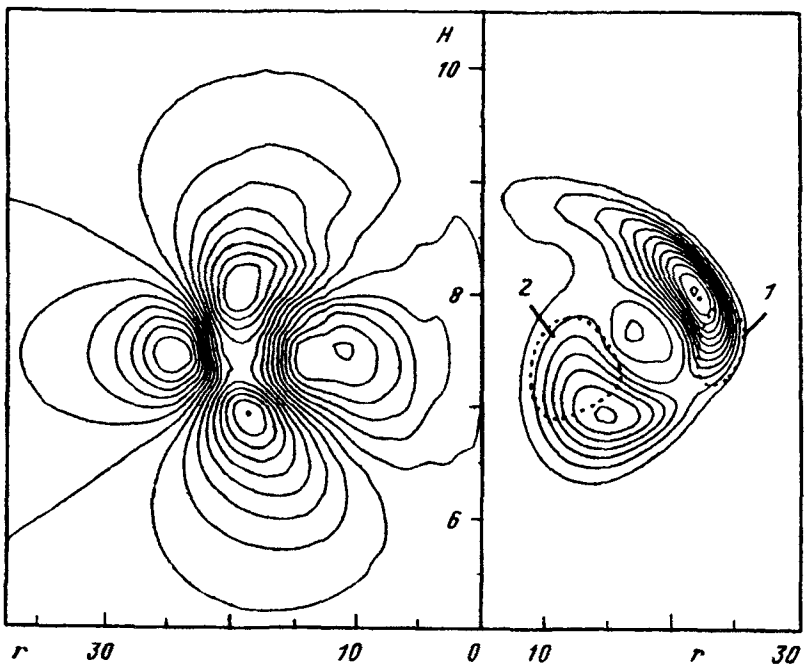

Fig. 3. Isolines of: components of the average strain-rate tensor (t=80 s) (*a*) and the Reynolds stresses (1 and 2 correspond to the region of contragradient transport). The axes are marked out in km.

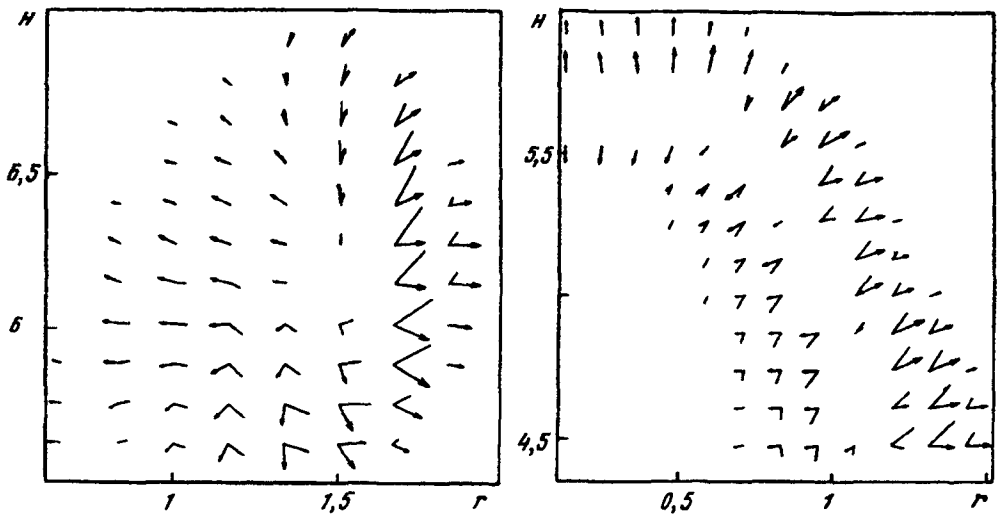

Fig. 5. Vector fields of the turbulent flux (with arrow heads) and the temperature gradient (*a* and *b* correspond to $t=30$ and 50 s). The axes are marked out in km.

Summary. The significant difference between the results of calculating the temperature-vortex torus cooling process reveals the limitations of the models which do not take into account the effect of flow rotation on the turbulent transport for flows of this type. Our investigation shows that taking the anisotropic effects into account is essential in simulating the turbulent gas flow in the thermal. The work done by the centrifugal forces in the vortex ring leads to the suppression of the turbulent transport in the radial direction. As a result, the isotropic local turbulence models, including the k–ε-model, lead to the overestimation of the effect of the dissipative processes caused by turbulence. Consequently, the values of many average parameters obtained from model 4 are closer to the "inviscid" as compared with those for the k–ε-model. The nonlinear k–ε-model usually gives results similar to those obtained from model 2. Therefore, the latter model, which is simpler than the others, can be used for investigating turbulent motions of the gas in ascending thermals. At the same time, in the stage of formation of the developed vortex flow model 3 overestimates the suppression of the turbulent transport.

The research was carried out with support from the Russian Foundation for Basic Research (project No. 95-01-00544a).

REFERENCES

1 C du P. Donaldson, "Calculation of turbulent shear flows for atmosphere and vortex motions," *AIAA J*, **10**, 4 (1972)
2 V B Levin, "Stabilizing effect of flow rotation on turbulence," *Teplofiz Vysok Temp*, **2**, 892 (1964)
3 Yu S Rusakov, "Experimental investigations of the structure and mass transfer of a turbulent vortex ring," *Zh Prikl Mekh Tekh Fiz*, No 4, 107 (1991)
4 A P. Darintsev, V N Zabavin, B V Zamyshlyaev et al, "Features of the motion of a heated, initially spherical air mass in the atmosphere," in: *Topical Problems of Continuum Mechanics* [in Russian], Moscow Physical and Technical Institute, Moscow (1985), p 126
5 A V Konyukhov, M V Meshcheryakov, and S V Utyuzhnikov, "Motion of a large-scale turbulent thermal in a stratified atmosphere," *Teplofiz Vysok Temp*, **32**, 236 (1994)
6 A V Konyukhov, M V Meshcheryakov, S V Utyuzhnikov, and L A Chudov, "Numerical simulation of a turbulent large-scale thermal," *Izv. Ros Akad Nauk, Mekh Zhidk Gaza*, No 3, 93 (1997)
7 B E Launder, G J Reece, and W Rodi, "Progress in the development of a Reynolds-stress turbulence closure," *J Fluid Mech*, **68**, 537 (1975)
8 A F Kurbatskii, *Simulation of Nonlocal Turbulent Momentum and Heat Transport* [in Russian], Nauka, Novosibirsk (1988)
9 Ya A Gistintsev, A F Solodovnik, V V Lazarev, Yu V Shatskikh, *Turbulent Thermal in a Stratified Atmosphere* [in Russian], Preprint of the Institute of Chemical Physics of the USSR Academy of Sciences, Chernogolovka (1985)
10 A T Onufriev, *Description of Turbulent Transport: Nonequilibrium Models* [in Russian], Moscow Physical and Technical Institute, Moscow (1995)
11 S W Park and M K. Chung, "Curvature-dependent two-equation model for prediction of turbulent recirculating flows," *AIAA J*, **27**, 340 (1987)
12 A V Konyukhov, M V Meshcheryakov, and S V Utyuzhnikov, "Numerical simulation of the flow initiated in the atmosphere by a near-ground turbulent thermal," *Teplofiz Vysok Temp*, **33**, 726 (1995)

13 H C Yee, R. F Warming, and A Harten, "Implicit total variation diminishing (TVD) schemes for steady-state calculations," *J Comp Phys*, **57**, 327 (1985)
14 M V Meshcheryakov, *Mathematical Simulation of Certain Gas Flows Initiated by a Point Explosion* [in Russian], Thesis for Degree of Candidate of Physico-Mathematical Sciences, Moscow Physical and Technical Institute, Moscow (1995)
15 M A Leschziner and W Rodi, "Calculation of annular and twin parallel jets using various discretization schemes and turbulence-model variations," *Trans ASME, J Fluids Enging*, **103**, 352 (1981)